



# Arginine 54 in the active site of *Escherichia coli* aspartate transcarbamoylase is critical for catalysis: A site-specific mutagenesis, NMR, and X-ray crystallographic study

JEFFREY W. STEBBINS,<sup>1</sup> DIANE E. ROBERTSON,<sup>1</sup> MARY F. ROBERTS,<sup>1</sup>  
RAYMOND C. STEVENS,<sup>2</sup> WILLIAM N. LIPSCOMB,<sup>2</sup> AND EVAN R. KANTROWITZ<sup>1</sup>

<sup>1</sup> Department of Chemistry, Merkert Chemistry Center, Boston College, Chestnut Hill, Massachusetts 02167

<sup>2</sup> Department of Chemistry, Gibbs Laboratory, Harvard University, 12 Oxford Street, Cambridge, Massachusetts 02138

(RECEIVED May 27, 1992; REVISED MANUSCRIPT RECEIVED June 26, 1992)

## Abstract

The replacement of Arg-54 by Ala in the active site of *Escherichia coli* aspartate transcarbamoylase causes a 17,000-fold loss of activity but does not significantly influence the binding of substrates or substrate analogs (Stebbins, J.W., Xu, W., & Kantrowitz, E.R., 1989, *Biochemistry* 28, 2592–2600). In the X-ray structure of the wild-type enzyme, Arg-54 interacts with both the anhydride oxygen and a phosphate oxygen of carbamoyl phosphate (CP) (Gouaux, J.E. & Lipscomb, W.N., 1988, *Proc. Natl. Acad. Sci. USA* 85, 4205–4208). The Arg-54 → Ala enzyme was crystallized in the presence of the transition state analog *N*-phosphonoacetyl-L-aspartate (PALA), data were collected to a resolution limit of 2.8 Å, and the structure was solved by molecular replacement. The analysis of the refined structure (*R* factor = 0.18) indicates that the substitution did not cause any significant alterations to the active site, except that the side chain of the arginine was replaced by two water molecules. <sup>31</sup>P-NMR studies indicate that the binding of CP to the wild-type catalytic subunit produces an upfield chemical shift that cannot reflect a significant change in the ionization state of the CP but rather indicates that there are perturbations in the electronic environment around the phosphate moiety when CP binds to the enzyme. The pH dependence of this upfield shift for bound CP indicates that the catalytic subunit undergoes a conformational change with a *pK<sub>a</sub>* ~ 7.7 upon CP binding. Furthermore, the linewidth of the <sup>31</sup>P signal of CP bound to the Arg-54 → Ala enzyme is significantly narrower than that of CP bound to the wild-type catalytic subunit at any pH, although the change in chemical shift for the CP bound to the mutant enzyme is unaltered. <sup>31</sup>P-NMR studies of PALA complexed to the wild-type catalytic subunit indicate that the phosphonate group of the bound PALA exists as the dianion at pH 7.0 and 8.8, whereas in the Arg-54 → Ala catalytic subunit the phosphonate group of the bound PALA exists as the monoanion at pH 7.0 and 8.8. Thus, the side chain of Arg-54 is essential for the proper ionization of the phosphonate group of PALA and by analogy the phosphate group in the transition state. These data support the previously proposed proton transfer mechanism, in which a fully ionized phosphate group in the transition state accepts a proton during catalysis.

**Keywords:** allosteric enzyme; aspartate carbamoyltransferase; enzyme mechanism; mutant structure; *N*-phosphonoacetyl-L-aspartate; <sup>31</sup>P-NMR; site-specific mutagenesis

Reprint requests to: Evan R. Kantrowitz, Merkert Chemistry Center, Boston College, Chestnut Hill, Massachusetts 02167.

**Abbreviations:** T and R states, tense and relaxed states of the enzyme having low and high affinity, respectively, for the substrates; pam, phosphonoacetamide; mal, malonate; CP, carbamoyl phosphate; PALA, *N*-phosphonoacetyl-L-aspartate; R<sub>pam,mal</sub> structure, the X-ray structure of aspartate transcarbamoylase determined in the presence of pam and mal (Gouaux et al., 1990); R<sub>PALA</sub> structure, the X-ray structure of aspartate transcarbamoylase determined in the presence of PALA (Krause et al., 1987); Arg-54 → Ala, the mutant enzyme in which Arg-54 of the catalytic chain of aspartate transcarbamoylase has been replaced by Ala.

Aspartate transcarbamoylase (EC 2.1.3.2) catalyzes the reaction between CP and L-aspartate to form *N*-carbamoyl-L-aspartate and inorganic phosphate (Jones et al., 1955; Reichard & Hanshoff, 1956). The carbamoyl aspartate thus formed proceeds through the pyrimidine biosynthetic pathway ultimately leading to the formation of the pyrimidine nucleotides. In *Escherichia coli*, aspartate transcarbamoylase is an allosteric enzyme exhibiting homotropic cooperativity with respect to both substrates

(Gerhart & Pardee, 1962; Bethell et al., 1968), heterotropic inhibition by CTP (Yates & Pardee, 1956), which is enhanced by UTP (Wild et al., 1989), and heterotropic activation by ATP (Gerhart & Pardee, 1962, 1963; Bethell et al., 1968), the product of the parallel purine biosynthetic pathway.

The *E. coli* holoenzyme is composed of 12 polypeptide chains of two types. There are six 33,000-Da chains that exist as two trimers and six 17,000-Da chains that exist as three dimers. Each of the trimers contains three active sites shared across the boundary between two adjacent catalytic chains (Monaco et al., 1978; Krause et al., 1985; Robey & Schachman, 1985; Wentz & Schachman, 1987). Each of the smaller or regulatory chains contains one binding site for the regulatory nucleotides that is approximately 60 Å from the active site.

X-ray crystallography has been utilized to determine the structure of the enzyme in both the absence and presence of substrates, substrate analogs, and the regulatory nucleotides (Krause et al., 1987; Kim et al., 1987; Gouaux & Lipscomb, 1988, 1990; Ke et al., 1988; Gouaux et al., 1990; Stevens et al., 1991). In particular, the residues interacting with the substrates have been identified from structures of the enzyme determined in the presence of PALA, a bisubstrate analog (Krause et al., 1987; Ke et al., 1988) (see Kinemage 1), CP and succinate (Gouaux & Lipscomb, 1988), as well as pam and mal (Gouaux et al., 1990).

The binding of the substrates to one or more of the active sites causes the quaternary conformational change that converts the enzyme from the T to the R allosteric state. The T to R conformational change also results in significant reorientation of amino acid side chains that interact with the substrates (see Kinemage 2), thus creating the high activity, high affinity active site characteristic of the R state of the enzyme. Although the X-ray structures of the enzyme with active site ligands bound have identified the side chains interacting with the substrates, site-specific mutagenesis experiments have been necessary to distinguish those side chains that affect catalysis from those involved in substrate binding alone. Every side chain that interacts specifically with the substrates has now been replaced by at least one amino acid (Robey et al., 1986; Stebbins et al., 1989, 1990; Xu & Kantrowitz, 1989, 1991). However, these studies have not been able to identify a specific side chain acting as a general base or as a proton transfer agent in the catalytic mechanism. These results support the proposal of Gouaux et al. (1987) that there is a direct proton transfer between the amino group of aspartate and the leaving phosphate group.

Of all the side chains that interact with the substrates, the removal of Arg-54 results in the largest reduction in catalytic activity, approximately 17,000-fold for the holoenzyme and 72,000-fold for the isolated catalytic subunit (Stebbins et al., 1989). The guanidinium group of the side chain of Arg-54 interacts specifically with the anhy-

dride oxygen as well as a terminal phosphate oxygen of CP (Gouaux & Lipscomb, 1988). Even though these interactions seem to be involved in CP binding, the binding affinities of CP and PALA are altered only marginally by loss of these specific side chain contacts with Arg-54 (Stebbins et al., 1989). Thus, the side chain of Arg-54 seems to affect only catalysis and to contribute little to substrate binding. In order to better understand the function of the side chain of Arg-54, we report here both the X-ray structure of the Arg-54 → Ala enzyme in the presence of the transition state analog PALA, as well as NMR experiments monitoring the phosphorus of CP and of PALA bound to the catalytic subunits of wild-type and the Arg-54 → Ala enzymes.

## Results

### *Structure of the Arg-54 → Ala aspartate transcarbamoylase*

The Arg-54 → Ala enzyme, in the presence of PALA, crystallized in the P321 space group with unit cell dimensions of  $a = b = 122.3$  Å and  $c = 156.6$  Å. This is the same space group and almost identical unit cell dimensions as observed for the wild-type enzyme, crystallized either in the presence of PALA,  $a = b = 122.2$  Å,  $c = 156.2$  Å (Krause et al., 1987), pam and mal (Gouaux & Lipscomb, 1990), or CP and succinate (Gouaux & Lipscomb, 1988). The crystals of the Arg-54 → Ala enzyme diffracted to a resolution limit of between 2.6 and 2.8 Å depending upon the particular crystal. Using three crystals, a data set that was 98% complete was collected to 2.8 Å with 6.9-fold redundancy. Molecular replacement yielded a structure that was refined to an *R*-factor of 0.18. The root mean square (rms) deviation for bonds was 0.012 Å and that for angles was 3.1°.

### *Comparison of the wild-type and the Arg-54 → Ala aspartate transcarbamoylases*

On the quaternary level, the structure of the Arg-54 → Ala enzyme is very similar to the structure of the wild-type enzyme in the R-state. On the tertiary level, a comparison of the positions of the  $\alpha$ -carbons reveals that no substantial deviations occur between the  $\alpha$ -carbons of the mutant and the wild-type structures. For example, Figure 1 shows the deviations in  $\alpha$ -carbon positions for one of the catalytic chains between the mutant and wild-type structures. Except at the C-terminus of the catalytic chain, a region of poor electron density, the  $\alpha$ -carbon deviations are generally less than 0.85 Å, and the average rms deviations of  $\alpha$ -carbons is 0.24 Å. For the entire structure, the only places where deviations exceed 1 Å are in regions of poor electron density in both the wild-type and mutant structures, such as the 80s and 240s loop regions.

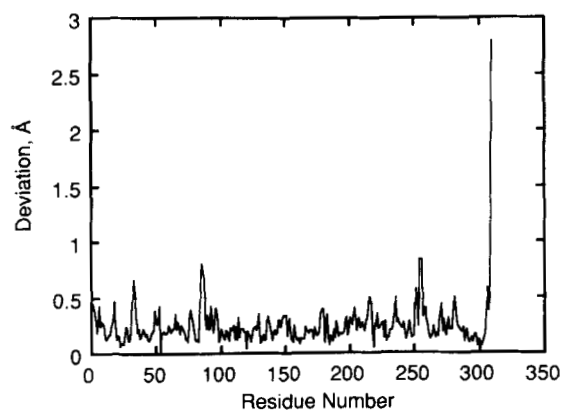


**Fig. 1.** The  $\alpha$ -carbon displacement between the Arg-54  $\rightarrow$  Ala enzyme complexed with PALA and the wild-type enzyme complexed with PALA (Ke et al., 1988). Shown are the distances for the C1 catalytic chain after superposition of the two structures.

The  $F_o - F_c$  electron-density map calculated after omission of the amino acid at position 54 in the catalytic chain is shown in Figure 2. The omit map clearly shows that electron density extends no further than the  $\beta$ -carbon of the side chain of residue 54. Therefore, the X-ray structure indicates that an alanine residue has replaced the arginine at position 54 in the mutant enzyme.

The omit map also showed a number of water molecules in the area of the active site. Those water molecules in the active site region having electron density at least  $3\sigma$  were added to the model during the final stages of refinement. Two of these water molecules were in positions previously occupied by the guanidinium nitrogens of Arg-54. Thus, the removal of Arg-54 from the active site of aspartate transcarbamoylase does not substantially alter the three-dimensional structure of the enzyme but does result in a more aqueous environment in the active site region (see Fig. 3 and Kinemage 3).

### $^{31}\text{P}$ studies of CP bound to the wild-type catalytic subunit

The chemical shift and linewidth of CP when bound to the catalytic subunit of the enzyme reflect the electronic environment of the phosphorus and are sensitive to even small conformational changes of the enzyme near the phosphorus. The high sensitivity is due to the fact that the  $^{31}\text{P}$  chemical shift of CP moves downfield  $\sim 5.3$  ppm ( $\sim 640$  Hz at this field strength) when the second phosphate hydrogen is removed ( $\text{p}K_a = 4.9$ ) (see Fig. 4A, inset). Even though, for most of the pH range used in the subsequent NMR studies with enzyme, free CP has an invariant chemical shift ( $-444$  Hz or  $-3.66$  ppm) and a  $-2$  charge, when wild-type catalytic subunit is added to form the catalytic subunit-CP complex the  $^{31}\text{P}$  signal of CP moves upfield. In two distinct regions the chemical shift is constant, although different from free CP (see Fig. 4A); below pH 7.5 the bound shift is  $-468$  Hz ( $-3.86$  ppm); and above pH 8.4 the bound shift is  $-452$  Hz ( $-3.72$  ppm). The change in the CP shift when bound to the catalytic subunit ( $0.2$  ppm upfield) cannot reflect a significant change in the ionization state of the ligand since protonation of the phosphate would yield a 5.3-ppm upfield shift. Although a detailed interpretation of this change in chemical shift upon ligand binding is not possible, it indicates that there are perturbations in the electronic environment around the phosphate moiety when CP binds to the enzyme. An upfield shift was previously observed for CP binding to the catalytic subunit at pH 7 (Roberts et al., 1976), although the magnitude differed somewhat from that observed in the present study. The pH dependence of the change in the chemical shift of bound CP indicates that the catalytic subunit undergoes a conformational change with a  $\text{p}K_a$  of  $\sim 7.7$ . Furthermore, the chemical shift of the bound CP on the high pH side of the  $\text{p}K_a$  is closer to that of free ligand in solution.

Evidence for such a conformational change that affects

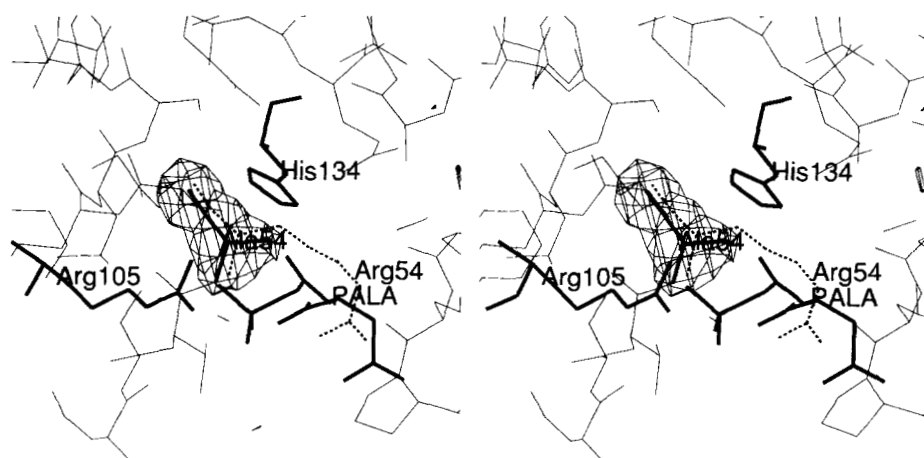


**Fig. 2.** Stereo view of the active site region of the Arg-54  $\rightarrow$  Ala enzyme. PALA and the side chains of His-134, Arg-105, and Ala-54 are shown in bold. In addition, the position of the Arg-54 side chain in the structure of the wild-type enzyme complexed with PALA is shown after superposition of the two structures (dashed line). Also shown is the electron-density map ( $F_o - F_c$ ), contoured at  $3.5\sigma$ , calculated with the Ala-54 residue omitted.

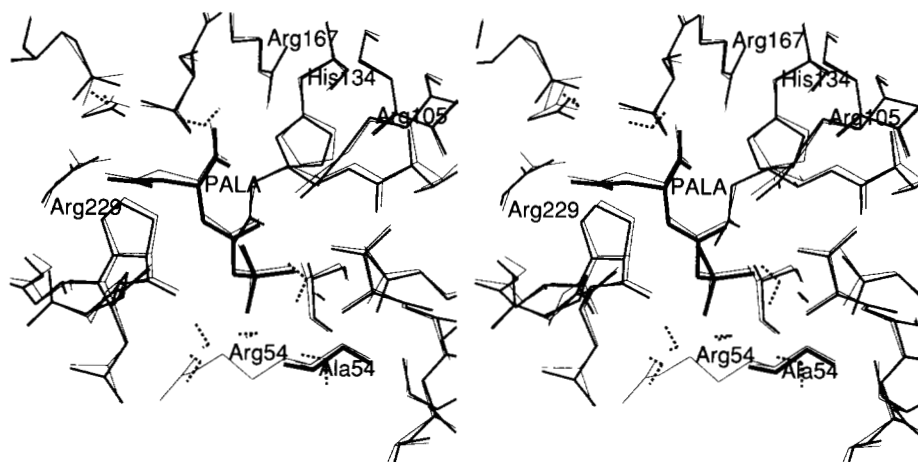


**Fig. 3.** Stereo view of the active site region of the wild-type (light) and the Arg-54 → Ala (dark) enzymes with PALA bound. The C1 catalytic chains of the wild-type and mutant structures were superimposed based on a rigid body least-squares alignment of the  $\alpha$ -carbons of the two structures. In the Arg-54 → Ala structure, residue 54 is shown in bold, and the water molecules (with hydrogens) in the active site region are shown with dashed lines.

the binding of CP can also be garnered from the linewidth, calculated for CP bound to the wild-type catalytic subunit. To a first approximation, one can assume fast exchange between the bound and free environments. The

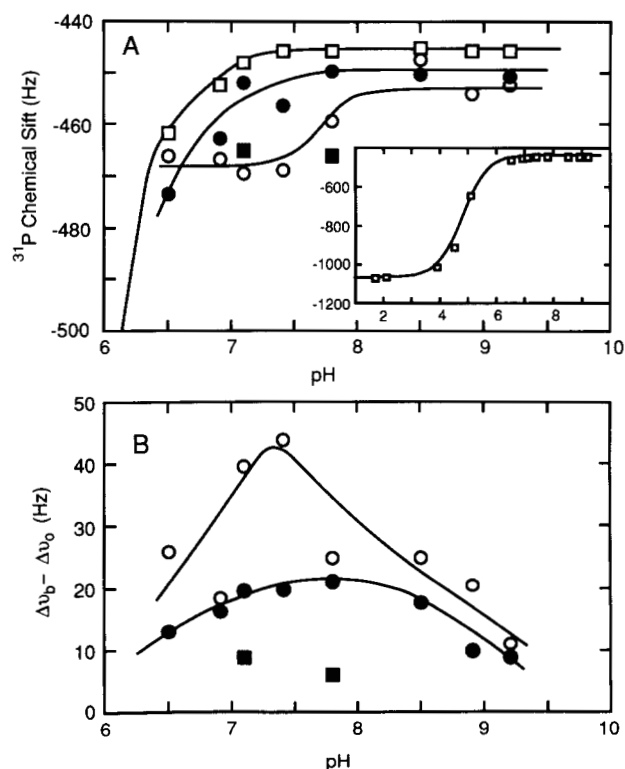


**Fig. 4.** The pH dependence of the CP  $^{31}\text{P}$  chemical shift (Hz from inorganic phosphate as zero) and linewidth (bound minus free). The inset in A shows the chemical shift of 20 mM CP and 50%  $\text{D}_2\text{O}$  as a function of pH. The CP (A) bound chemical shifts and (B) bound linewidths extrapolated from the observed  $^{31}\text{P}$  parameters as a function of the ratio of ligand to enzyme active sites (assuming fast exchange) are shown as a function of pH:  $\square$ , free ligand;  $\circ$ , CP bound to wild-type catalytic subunit;  $\blacksquare$ , CP bound to Arg-54 → Ala catalytic subunit;  $\bullet$ , CP bound to wild-type catalytic subunit in the presence of 10 mM succinate.

observed linewidth is then the weighted average of free and bound ligand linewidths. The pH dependence of this parameter for CP bound to the wild-type enzyme is shown in Figure 4B (open circles); a maximum in bound linewidth appears between pH 7 and 7.5. For fast exchange, the value of the bound linewidth that is extrapolated from this treatment has a term that includes the lifetime of the complex as well as  $T_2$ . If the exchange rate is slower, such that the system is in the intermediate exchange regime, further broadening of the observed resonance occurs. The bound linewidth is now described by a more complex expression with a term containing the square of the chemical shift for the bound ligand (Swift & Connick, 1962). Although the data include  $\sim 20\%$  error in the determination of these linewidths, one can easily see that the linewidth of the bound CP is a function of pH (see Fig. 4B). Below pH 7 and above pH 8.7 the increase in the linewidth from free to bound CP is  $\sim 20$  Hz. Between pH 7.5 and 8.5 the bound linewidth increases two-fold. The linewidth of the bound CP is largest where the chemical shift is greatest. Hence exchange broadening does contribute to the observed linewidth of CP.

#### *$^{31}\text{P}$ studies of CP bound to the Arg-54 → Ala catalytic subunit*

The Arg-54 → Ala catalytic subunit–CP complex exhibits similar  $^{31}\text{P}$  chemical shift behavior as a function of pH (Fig. 4A, filled squares), as does the wild-type catalytic subunit. However, the increased linewidth at  $\sim$ pH 7.5 is not observed (Fig. 4B, filled squares). In fact, the linewidth for CP bound to the Arg-54 → Ala catalytic subunit is significantly narrower than for the ligand bound to the wild-type catalytic subunit at any pH. The chemical shift is the same for CP bound to the wild-type and the Arg-54 → Ala catalytic subunits, whereas the linewidths are different, implying that the Arg-54 interactions with the phosphate group normally retard the exchange between the free and the bound forms of CP. Other groups

at the active site of the enzyme must be responsible for the change in the chemical shift upon CP binding and the altered electronic environment of the phosphate.

*<sup>31</sup>P studies of CP bound to the wild-type and Arg-54 → Ala catalytic subunits in the presence of succinate*

When 10 mM succinate is added to form a ternary complex with CP and the wild-type catalytic subunit, the chemical shift and linewidths no longer sense the conformational change of the catalytic subunit. The chemical shift (Fig. 4A, filled circles) is ~4 Hz upfield from that of free CP from pH 6.5 to 9, hence the electronic environment of bound CP in this complex is comparable to that of free CP in solution. The linewidth for bound CP in the presence of succinate does not show the increase at a pH of ~7.5 observed in the absence of succinate (Fig. 4B, filled circles). This behavior would be expected because in an intermediate exchange regime the chemical shift contributes to the observed linewidth, and the term for the chemical shift of CP has been significantly decreased, from 20 Hz to 4 Hz. The behavior of the chemical shift of CP bound to the Arg-54 → Ala and wild-type catalytic subunits is the same when succinate is added, and again the linewidth is significantly narrower in the mutant catalytic subunit, consistent with a transition to a fast exchange regime. In the ternary complex, there is no significant electronic difference between CP bound to the wild-type or to the Arg-54 → Ala catalytic subunits.

*<sup>31</sup>P studies of PALA bound to the wild-type catalytic subunit*

The active site environment during catalysis cannot be sensed with <sup>31</sup>P-NMR studies of CP and succinate bound to the enzyme, but it can be explored using the transition state analog PALA. The p*K<sub>a</sub>* of the PALA phosphonate group can be measured from the pH dependence of its <sup>31</sup>P chemical shift. As shown in Figure 5, over the pH range between 4 to 10 the chemical shift moves upfield by 2.2 ppm. The singly charged phosphonate has a characteristic chemical shift of 14.4 ppm, whereas the shift of the doubly ionized phosphonate is 12.2 ppm. From these data a p*K<sub>a</sub>* of 7.5 is extracted for generation of the dianionic form of the phosphonate group. A comparable p*K<sub>a</sub>* was derived from <sup>13</sup>C-NMR studies of PALA as a function of pH (Roberts et al., 1976).

If PALA is bound to the wild-type catalytic subunit and examined at pH 7 and pH 8.8, information should be provided on the ionization state of the bound phosphonate. In a similar fashion the ionization state of that group when bound to mutant catalytic subunit can also be determined and compared to the data for the wild-type catalytic subunit. The binding constant of PALA to the wild-type catalytic subunit is 27 nM (Collins & Stark, 1971). Given this tight binding, free and bound PALA are likely to be in

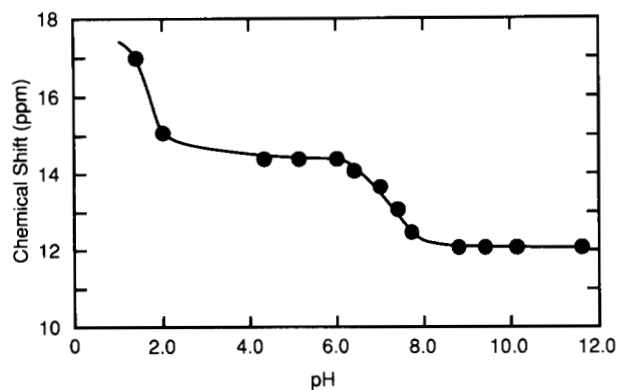
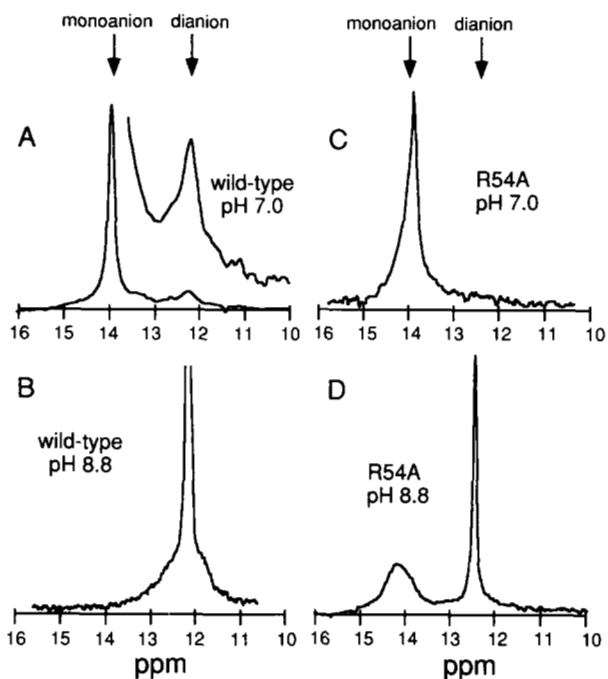


Fig. 5. The pH dependence of the PALA <sup>31</sup>P chemical shift between pH 2 and 12. Solutions containing approximately 20 mM PALA and 50% D<sub>2</sub>O were adjusted to various pH values with either NaOH or HCl at ambient temperature. After each pH adjustment the chemical shift was determined.

slow exchange and two discrete resonances should be detected. Upon the addition of 2 mM or higher concentrations of PALA to the wild-type catalytic subunit (1 mM in active sites) at pH 7 two resonances are observed: a narrow one ~14 ppm, which is the chemical shift of the free PALA at this pH, and a second broader resonance at 12.2 ppm, the chemical shift of the completely ionized bound phosphonate (see Fig. 6A). The linewidth of the bound PALA is ~80 Hz, indicating that the phosphonate group is significantly immobilized (free PALA has a linewidth of ~5 Hz under these conditions). When the wild-type catalytic subunit is incubated with PALA at pH 8.8, both the sharp (free) and broader (bound) resonances overlap (see Fig. 6B) at 12.2 ppm, the chemical shift for the doubly ionized species. Therefore, at either pH 7.0 or 8.8, when PALA is bound to the wild-type catalytic subunit it exists with its phosphonate group fully ionized. Slow exchange of free and bound PALA <sup>31</sup>P resonances at pH 7.0 has been observed previously (Cohen & Schachman, 1986), and the chemical shift of the bound PALA phosphonate indicated it was bound as the dianion. In earlier studies with <sup>13</sup>C-carbonyl-labeled PALA bound to the catalytic subunit at pH 7, slow exchange was also observed with a downfield shift for the enzyme-bound species (Roberts et al., 1976). Interpretation in these earlier studies of the <sup>13</sup>C shift was ambiguous because the phosphonate ionization could not be distinguished from hydrogen bonding to the carbonyl. In light of these <sup>31</sup>P experiments, the <sup>13</sup>C PALA shift can be reinterpreted as arising from a preference of the catalytic subunit for the doubly ionized phosphonate group of PALA.

*<sup>31</sup>P studies of PALA bound to the Arg-54 → Ala catalytic subunit*

The Arg-54 → Ala catalytic subunit also shows slow exchange between free and bound PALA on the NMR



**Fig. 6.**  $^{31}\text{P}$  (121.4 MHz) spectra of wild-type (A, B) and Arg-54  $\rightarrow$  Ala (C, D) catalytic subunits (1 mM in active sites) in the presence of (A) 1.5 mM PALA, pH 7 (line broadening = 10 Hz); (B) 2 mM PALA, pH 8.8 (line broadening = 4 Hz); (C) 2 mM PALA, pH 7 (line broadening = 4 Hz); and (D) 2 mM PALA, pH 8.8 (line broadening = 10 Hz). In A an expanded scale trace is also shown for the region between 13.5 and 10 ppm. The  $^{31}\text{P}$  chemical shift of PALA is approximately 14.4 ppm and 12.2 ppm when it exists as the monoanion and dianion, respectively (see Fig. 5).

time-scale. When the Arg-54  $\rightarrow$  Ala catalytic subunit is at pH 7, both free and bound PALA have a chemical shift of approximately 14 ppm, hence the bound phosphonate group has a single negative charge (see Fig. 6C). The observed resonance with overlapping free and bound PALA is asymmetric, indicating that the free and bound species have slightly different chemical shifts. The sharp (free) PALA resonance is slightly upfield, consistent with the fact that at this pH some doubly charged phosphonate is in fast exchange with the singly charged free species. At pH 8.8, while free PALA exists with a doubly ionized phosphonate, the chemical shift of the bound PALA is observed at approximately 14 ppm, indicating that the phosphonate is singly ionized (see Fig. 6D). Therefore, the replacement of the arginine with an alanine has dramatically altered the ionization state of the enzyme-bound PALA.

## Discussion

Site-specific mutagenesis has been used extensively to probe the active site of aspartate transcarbamoylase. In fact, every one of the side chains that forms specific interactions with the substrates has been replaced one or

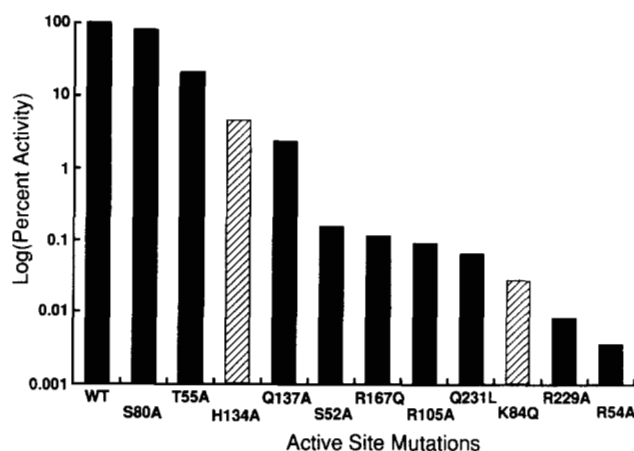


**Fig. 7.** Comparison of activity of wild-type (WT) aspartate transcarbamoylase holoenzyme with single amino acid substitution mutants in the active site of the enzyme. For the mutant enzymes, the one-letter amino acid code before the residue number corresponds to the amino acid in the wild-type enzyme, and the one-letter amino acid code after the residue number corresponds to the amino acid in the mutant enzyme. The activities of each of the enzymes were calculated as a percentage of the wild-type activity under the particular conditions reported and plotted here as the log. The data for the H134A and K84Q enzymes were obtained at pH 7.0 (Robey et al., 1986), and the data for the S80A, S52A (Xu & Kantrowitz, 1991), T55A (Xu & Kantrowitz, 1989), the Q137A, R105A, R54A (Stebbins et al., 1989), the R167Q, Q231L (Stebbins et al., 1990), and the R229A (Middleton et al., 1989) enzymes were determined at pH 8.3.

more times (Robey et al., 1986; Stebbins et al., 1989, 1990; Xu & Kantrowitz, 1989, 1991) (see Fig. 7), and their role in catalysis has been inferred (see Table 2). The replacement of Arg-54 by alanine results in a reduction in maximal velocity of 17,000-fold and 72,000-fold for the mutant holoenzyme and catalytic subunit, respectively (see Table 1 and Stebbins et al. [1989]). The side chain of Arg-54

**Table 1.** Comparison of the kinetic parameters of the wild-type and the Arg-54  $\rightarrow$  Ala enzymes at pH 8.3<sup>a</sup>

Holoenzyme	$V_{max}^b$ (mmol $\cdot$ h <sup>-1</sup> $\cdot$ mg <sup>-1</sup> )	$[S]_{0.5}^{ASP}$ (mM)	$[S]_{0.5}^{CP}$ (mM)	$n_H^{ASP}$	$n_H^{CP}$
Wild type	17	11.8	0.2	2.2	2.0
Arg-54 $\rightarrow$ Ala	0.001	26	0.2	1	1
Catalytic subunit	$V_{max}$ (mmol $\cdot$ h <sup>-1</sup> $\cdot$ mg <sup>-1</sup> )	$K_m^{ASP}$ (mM)	$K_m^{CP}$ (mM)	$k_{cat}/K_m^{ASP}$ (s <sup>-1</sup> $\cdot$ mM <sup>-1</sup> )	
Wild type	25.9	6.7	0.02	37.2	
Arg-54 $\rightarrow$ Ala	0.00036	8.3	0.09	0.0004	

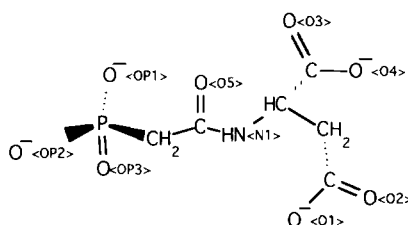
<sup>a</sup> Kinetic data were determined in 0.05 M Tris-acetate buffer pH 8.3 at 25  $^{\circ}\text{C}$  for the wild-type and the Arg-54  $\rightarrow$  Ala holoenzymes and catalytic subunits (Stebbins et al., 1989).

<sup>b</sup>  $V_{max}$  represents the maximal observed specific activity from the aspartate saturation curve.

**Table 2.** Role of active site residues in catalysis

Protein	Interaction <sup>a</sup>	Proposed function	Mutation	Reference
Ser-52 OG	OP1	Orient CP	S52F S52H S52A	Robey et al., 1986 Wente & Schachman, 1987 Xu & Kantrowitz, 1991
Thr-53 NH	OP2	Neutralize PO <sub>4</sub> <sup>-</sup>		
Arg-54 NH	OP2	Neutralize PO <sub>4</sub> <sup>-</sup> , promote release of PO <sub>4</sub> <sup>-</sup> from transition state	R54A	Stebbins et al., 1989
Arg-54 NH1	OP2			
Arg-54 NE	OP2			
Thr-55 NH	OP3	Polarize CO of CP	T55A	Xu & Kantrowitz, 1989
Thr-55 OG1	OP3, O5			
Arg-105 NH1	OP1	Polarize CO of CP	R105A	Stebbins et al., 1989
Arg-105 NH1	OP3	Neutralize PO <sub>4</sub> <sup>-</sup>		
Arg-105 NH2	O5			
His-134 NE2	O5	Polarize CO of CP	H134A	Robey et al., 1986
Gln-137 OE2 <sup>b</sup>	N1	Polarize CO of CP	Q137A	Stebbins et al., 1989
Arg-167 NH2	O3	Orient transition state	R167Q	Stebbins et al., 1990
Arg-229 NE	O1, O2	Binding and stabilization of the transition state	R229A	Middleton et al., 1989
Arg-229 NH1	O2			
Gln-231 NE2	O1	Orient aspartate, cooperativity	Q231L	Stebbins et al., 1990
Lys-84 NZ	OP1	Cooperativity, neutralize PO <sub>4</sub> <sup>-</sup>	K84Q K84R	Robey et al., 1986 Robey et al., 1986
Ser-80 OG	OP1	Cooperativity	S80A	Xu & Kantrowitz, 1991
Pro-266 O	N1	Orient aspartate		
Leu-267 O	N1	Orient aspartate		

<sup>a</sup> Interactions between aspartate transcarbamoylase and PALA are based on the R<sub>PALA</sub> structure (Ke et al., 1988). The abbreviations used for the atoms of the PALA molecule are shown below.



<sup>b</sup> Differences between PALA ligation and CP + succinate ligation are observed near Gln-137 (Gouaux & Lipscomb, 1988).

interacts specifically with the anhydride oxygen as well as a terminal phosphate oxygen of CP (Gouaux & Lipscomb, 1988). Nevertheless, the replacement of Arg-54 does not substantially alter the binding of CP or the bisubstrate analog PALA (see Table 1 and Stebbins et al. [1989]). The relatively unaltered binding of substrates and substrate analogs suggests either that the side chain of Arg-54 is not strongly involved in substrate binding, that its contribution to binding is compensated by the displacement of water from the active site as the substrate binds, or that it serves a catalytic function in the transition state. Therefore, to further evaluate the role of the side chain of Arg-54 in the catalytic mechanism of aspartate transcarbamoylase we have performed additional studies on the Arg-54 → Ala enzyme by X-ray crystallography and by <sup>31</sup>P-NMR.

### The three-dimensional structure of the Arg-54 → Ala enzyme

In order to verify that the replacement of Arg-54 by alanine did not induce any substantial alterations to the three-dimensional structure, which could lead to loss of activity, the structure of the Arg-54 → Ala enzyme complexed with PALA was determined to 2.8 Å resolution. Comparison of the wild-type and the Arg-54 → Ala structures reveals that the replacement of Arg-54 by alanine does not cause any substantial alterations to the three-dimensional structure of the enzyme. The average rms deviation of α-carbons between the mutant and wild-type structures is 0.24 Å and 0.52 Å for the catalytic and regulatory chains, respectively. As seen in Figure 3 and Kinemage 3, the active site regions of the two structures are

virtually identical except for the actual replacement of Arg-54 by alanine in the mutant structure and for an alteration in the water structure in the active site. The cavity left by the loss of the side chain of Arg-54 is partially filled by two ordered water molecules that are positioned near the location of the guanidinium nitrogens of Arg-54.

#### *CP binding site*

$^{31}\text{P}$  NMR experiments indicate that the ionic environment near the phosphate group of bound CP is similar for both the wild-type and Arg-54  $\rightarrow$  Ala catalytic subunits. Analysis of the chemical shift of bound CP indicates that a conformational change, which alters the phosphate environment, occurs in the wild-type catalytic subunit when CP binds. The same conformational change is sensed by  $^{31}\text{P}$ -NMR when CP binds to the Arg-54  $\rightarrow$  Ala catalytic subunit. However, the phosphate group of CP was seen to have greater mobility in the Arg-54  $\rightarrow$  Ala enzyme-CP complex than in the wild-type enzyme-CP complex. If the phosphate group of CP is acting as a general base in the reaction, then the side chain of Arg-54 may stabilize a catalytically important orientation of the substrate. In the crystal structure of the Arg-54  $\rightarrow$  Ala holoenzyme in the presence of PALA several water molecules replace the arginine side chain, but it is unlikely that these are sufficient to orient CP in the same fashion. The above results suggest that the side chain of Arg-54 functions in the wild-type active site to stabilize the phosphate group of CP in a position and with a state of ionization that may be important for catalysis.

#### *The effective ionic environment of the Arg-54 $\rightarrow$ Ala and wild-type active sites*

In order to probe further the interactions of PALA with the wild-type and the Arg-54  $\rightarrow$  Ala enzymes,  $^{31}\text{P}$ -NMR spectroscopy was utilized. Although the physical location of bound PALA is the same, the interaction of PALA with these two enzymes is quite different. In the case of the wild-type enzyme, bound PALA exists as a dianion at both pH 7.0 and pH 8.8 (see Fig. 6A,B). Although the dianion would be the expected form in solution at pH 8.8, at pH 7.0 the predominant form of PALA would be the monoanion (see Fig. 5). For the Arg-54  $\rightarrow$  Ala enzyme the situation is different. At pH 7.0, the bound PALA exists as the monoanion as would be expected based on the ionization of free PALA in solution; but at pH 8.8, the bound PALA still exists as the monoanion (see Fig. 6C,D), even though free PALA exists as the dianion at this pH (see Fig. 5). Therefore, the wild-type enzyme is stabilizing the bound PALA as the dianion at both pH values, whereas the mutant is stabilizing the bound PALA as the monoanion also at both pH values. The observation that PALA binds to the enzyme as the dianion at pH 7.0 confirms pre-

vious experiments by NMR (Cohen & Schachman, 1986) and potentiometry (Allewell et al., 1979).

The above experiments demonstrate that the replacement of Arg-54 by an alanine dramatically alters the  $\text{p}K_a$  of the phosphonate group of PALA in the enzyme-ligand complex. The ionic environment about the phosphonate group of the bisubstrate analog PALA should closely reflect the ionic environment of the active site during catalysis. A proposed decrease in  $\text{p}K_a$  of the phosphate group of CP during catalysis is the only physical/structural alteration in the extremely low activity Arg-54  $\rightarrow$  Ala enzyme, as compared to the wild-type enzyme. The above results indicate that the side chain of Arg-54 functions in the wild-type active site to create an ionic environment that is important for catalysis.

Although the electronic microenvironment is similar for CP bound to both enzymes, the  $^{31}\text{P}$ -NMR studies showed greater mobility of the phosphate group of CP when bound to the Arg-54  $\rightarrow$  Ala catalytic subunit. In the crystal structure of the wild-type enzyme, determined with CP and succinate bound (Gouaux & Lipscomb, 1988), Arg-54 interacts with a phosphate oxygen and the anhydride oxygen. If intramolecular proton transfer to either (or both) of these is necessary for catalysis, and Arg-54 stabilizes a particular orientation and ionization state of the substrate, then replacement of the Arg-54 side chain would cause a significant drop in catalytic efficiency. In the crystal structure of the Arg-54  $\rightarrow$  Ala enzyme two water molecules replace the guanidinium portion of the arginine side chain, but it is unlikely that these are sufficient to orient CP in the same fashion. Therefore, the alteration in the ionic environment (including the state of ionization) and/or the greater mobility of the phosphate of CP, upon the replacement of Arg-54 by Ala, can be used to rationalize the greatly reduced activity of the Arg-54  $\rightarrow$  Ala enzyme.

#### *Catalysis*

Based on the results reported here, as well as many previous studies, more details of the catalytic mechanism can now be described. The binding of the substrates, CP and aspartate, to aspartate transcarbamoylase is ordered such that CP binds before aspartate (Porter et al., 1969; Wedler & Gasser, 1974; Hsuanyu & Wedler, 1987). The  $^{31}\text{P}$ -NMR experiments reported here provide additional evidence for conformational changes associated with the binding of CP, effects of which have also been observed by CD (Griffin et al., 1972), sedimentation (Kirshner & Schachman, 1971, 1973), and UV difference spectroscopy (Collins & Stark, 1969). In addition, the structure of the T form bound to pam shows the conformational changes due to the binding of an analog of CP (Gouaux & Lipscomb, 1990). The importance of conformational changes for the binding of aspartate and for catalysis has been ascertained from site-specific mutations in the CP binding



site. Mutations of Thr-55 → Ala (Xu & Kantrowitz, 1989), Arg-105 → Ala (Stebbins et al., 1989), Gln-137 → Ala (Stebbins et al., 1989), and Ser-52 → Ala (Xu & Kantrowitz, 1991) all alter the conformational changes associated with CP binding, and, moreover, the mutant enzymes have significantly reduced catalytic activity and affinity for aspartate. Thus, the binding of CP and the associated conformational changes not only result in activation of CP but also create the binding site for aspartate.

The binding of aspartate to the enzyme-CP complex also induces a conformational change, which has been observed by sedimentation studies (Kirshner & Schachman, 1971, 1973; Howlett & Schachman, 1977), ultraviolet difference spectroscopy (Collins & Stark, 1969, 1971), circular dichroism (Griffin et al., 1973), and directly by crystallography using substrate analogs (Gouaux & Lipscomb, 1988; Ke et al., 1988; Gouaux et al., 1990) (see Kinemage 4). On the tertiary level this conformational change results in the closure of the two domains of the catalytic chain, and orientation of residues such as Arg-229, Arg-167, Gln-231 and Lys-84 into their catalytically active positions (Gouaux & Lipscomb, 1990; Gouaux et al., 1990; Stevens et al., 1990) (see Kinemage 2). The X-ray structural data (Ke et al., 1988) and the NMR experiments with PALA reported here suggest that in the transition state the phosphate of CP is held very tightly in the active site of the enzyme by specific interactions that are capable of effectively distributing or neutralizing the charge on the dianionic CP (see Fig. 8). This charge neutralization would also dramatically enhance the leaving

group potential of the phosphate. Other groups in the active site such as His-134, Arg-105, Thr-55, and perhaps Gln-137 are all involved in activating the carbonyl carbon for nucleophilic attack by aspartate. However, in order for nucleophilic attack to occur, aspartate at physiological pH must lose one amino proton prior to or during catalysis. In enzymic catalysis, deprotonation of substrates is generally accomplished by two mechanisms: first, proton transfer to a functional group or groups on the enzyme; second, exclusive binding of the deprotonated form of the substrate. Coincident with the former case is a pH-dependent substrate binding, in which there is a change in substrate affinity at pH values near the  $pK_a$  or  $pK_a$ 's of a group or groups involved in proton transfer. Kinetic experiments, which determined affinity constants of the wild-type and His-134 → Asn enzymes for aspartate and succinate as a function of pH, suggest that aspartate is not deprotonated by the enzyme-CP complex (Xi et al., 1990). Therefore, the amino group of aspartate may be bound in a deprotonated form.

Following aspartate binding, catalysis has been proposed to proceed through a tetrahedral intermediate about the carbonyl carbon (Gouaux et al., 1987). As seen in Figure 8, the breakdown of this tetrahedral intermediate requires the loss of one proton to make the amide. Although the disposition of the first proton that is lost from aspartate ( $^+H_3N- \rightarrow H_2N-$ ) is uncertain, the transfer of the second proton directly to the leaving phosphate would efficiently neutralize the charge being formed on the leaving group. If the phosphate group in the above mechanism

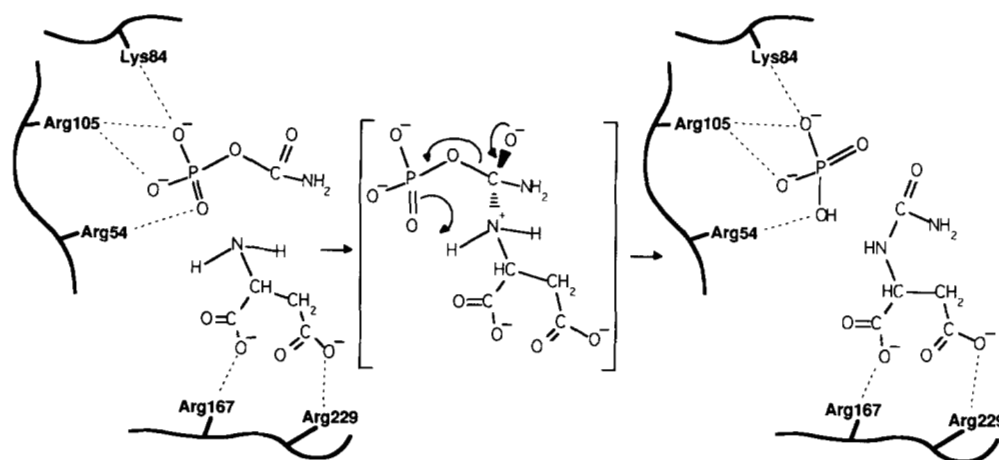


**Fig. 8.** Schematic diagram of the catalytic mechanism of aspartate transcarbamoylase. Only those side chains involved in charge neutralization of either the phosphate of CP or the carboxylates of aspartate are indicated specifically. The binding of CP to the CP domain of the catalytic chain induces conformational changes that allow the high affinity binding of aspartate. The binding of aspartate to the aspartate domain of the catalytic chain induces both tertiary and quaternary conformational changes resulting in the conversion of the enzyme from the T to the R state. The positive charges surrounding the phosphate of CP neutralize its charge. The  $^{31}P$ -NMR experiments indicate that PALA binds to the wild-type enzyme as the dianion at pH 7 even though in free solution PALA exists as the monoanion. Site-specific mutagenesis experiments have failed to identify any side chains in the active site region acting as a general base. These results, in conjunction with the NMR data reported here, add additional support the mechanism proposed by Gouaux et al. (1987) that there is a direct transfer of a proton from the amino group of aspartate to the phosphate leaving group in the tetrahedral intermediate.

is acting as a general base, then its protonation state may influence the rate of both the breakdown of the catalytic intermediate and the overall reaction. The transfer of the aspartate proton directly to the leaving phosphate is supported by site-specific mutagenesis and other experiments that have failed to identify a residue in the active site of the enzyme that could act as a general base to accept the proton from the aspartate.

What is the  $pK_a$  of the phosphate group in the tetrahedral intermediate? To a first approximation, the  $pK_a$  of this phosphate group should lie between the  $pK_a$  of the substrate and  $pK_a$  of the product, i.e., the  $pK_a$  of the monoanion of CP ( $pK_a = 4.9$ ) and the  $pK_a$  of the monoanion inorganic phosphate ( $pK_a = 7.2$ ), respectively. The stabilization of the more protonated forms of ligands containing phosphate in the Arg-54 → Ala enzyme, in contrast to the behavior of the wild-type enzyme, implies some degree of protonation of the phosphate in the tetrahedral intermediate. The observed change in the environment near the phosphate of the tetrahedral intermediate and the possible protonation of its phosphate group provides a rationale for the extremely low activity of the Arg-54 → Ala enzyme. Similarly, the substitution of an alanine for Arg-54, which concomitantly causes extreme low activity and protonation of the phosphate group, if extrapolated to the tetrahedral intermediate, lends strong support to the mechanism of intramolecular proton proposed by Gouaux et al. (1987). Further studies are needed however to establish to what degree the steps in the reaction are consecutive or concerted.

In summary, the  $^{31}\text{P}$ -NMR results reported here indicate that Arg-54 is crucial in binding and immobilizing the phosphate moiety when CP is the sole ligand of the enzyme. Arg-54 is also critical for maintaining the high negative charge on the phosphate group in a pseudotransition state. If Arg-54 has the same function in the actual transition state, it presumably makes the phosphate group an acceptor for intramolecular transfer of an aspartate proton in the reaction.

## Materials and methods

### Chemicals

CP,  $\text{D}_2\text{O}$ , L-aspartate, potassium dihydrogen phosphate, imidazole, maleic acid, sodium azide, N-ethylmorpholine, and Tris were purchased from Sigma. The CP was purified by precipitation from 50% (v/v) ethanol and stored desiccated at  $-20^\circ\text{C}$  (Gerhart & Pardee, 1962). PALA was a gift of the National Cancer Institute.

### Enzyme purification

The wild-type and Arg-54 → Ala holoenzyme and catalytic subunits were purified as previously described (Stebbins et al., 1989).

### Crystal growth, data collection, and reduction

Crystals of the Arg-54 → Ala aspartate transcarbamoylase were grown in the presence of PALA under the conditions previously reported (Krause et al., 1987). Hexagonal bars with approximate dimensions of  $0.6 \times 0.6 \times 2$  mm grew after about 1 week.

Collection of the diffraction data was accomplished using the Crystallographic Facility in the Chemistry Department of Boston College. One multiwire proportional chamber (Hamlin et al., 1981) was used and the  $\text{CuK}\alpha$  radiation was obtained with a graphite monochromator. Data were collected using the San Diego Multiwire MARK III system, which was driven by a Micro VAX3500 computer and linked to a Rigaku RU-200 rotating-anode generator operated at 50 kV and 150 mA.

In the data collection process, the crystals were mounted in sealed glass capillaries and aligned on a goniostat. The detector was set at a distance of 78 cm from the crystal, and a helium pathway was employed between the detector and the crystal to eliminate the effects of air scattering. The intensities of diffraction maxima were measured using an  $\omega$  scan at stepsize intervals of  $0.1^\circ$ . The radiation damage and crystal decay were calculated using a ratio of the averaged intensity for the same diffraction zone at an initial time and a later time. A crystal was replaced when the relative decay of the average intensity was 16% or greater. The distance between the detector and the crystals permitted measurement of diffraction maxima to 2.73 Å resolution. Of the 33,922 unique reflections possible to 2.8 Å, 33,351 reflections were collected with an average redundancy of 6.9. Data analysis was accomplished using the software provided by San Diego Multiwire (Howard et al., 1985). After correction for Lorentz and polarization effects, the symmetry-related reflections were identified according to the space group P321 and were merged together and sorted. A scale factor was calculated for multiple measurements and symmetry-related reflections. Those measurements deviating substantially from the average for a particular reflection were manually deleted. This scaling and editing procedure was repeated until the scaling  $R$ -factor converged.

The crystal structure was solved by using the molecular replacement method, employing as the initial model the  $R_{\text{pam,mal}}$  structure (Gouaux & Lipscomb, 1990) with the pam, mal, solvent, and the side chain of residue 54 deleted. This structure was used because it was the best structure of the R state of the enzyme available at the time. The initial  $R$ -factor was 0.26. After positional refinement, simulated annealing was employed followed by Powell minimization using the program XPLOR (Polygen Corporation) running on an IBM RISC/6000 computer. Electron-density maps were calculated ( $F_o - F_c$ ), and the PALA molecule was built into the electron density at the active site starting initially with the coordinates of PALA from the  $R_{\text{PALA}}$  structure (Krause et al., 1987) using the

structural analysis and refinement (STAR) software that is part of QUANTA (Polygen Corporation). At this stage, two to three water molecules were also placed in density in the active site region. After positional refinement (100 steps) and restrained *B*-factor refinement using XPLOR, electron density maps ( $2F_o - F_c$ ) as well as omit maps ( $F_o - F_c$ ) with residue 54 omitted were calculated. After additional water molecules were added to the active site region, the model was subjected to two cycles of refinement; each cycle consisted of positional refinement (100 steps) followed by restrained *B*-factor refinement. The final *R*-factor was 0.18.

#### NMR sample preparation

Prior to NMR spectroscopy the enzymes were exhaustively dialyzed into either 100 mM imidazole-acetate or 100 mM Tris-acetate buffers, which contained 2 mM 2-mercaptoethanol and 0.2 mM EDTA. The pH range of these buffers varied from 6.5 to 8.9. Following dialysis the enzyme samples were concentrated using a Amicon microconcentrator in a clinical centrifuge. After determination of protein concentration, the enzymes were then diluted into the buffers described above. These buffers also contained 20–50% D<sub>2</sub>O and in some cases PALA or succinate. Final concentrations in these samples ranged from 1 mM to 2 mM in active sites, 1.5 to 5 mM in PALA, and 10 mM in succinate. In some cases microliter aliquots from a buffered solution of 20 mM CP were added during NMR spectral acquisition.

#### NMR spectroscopy

<sup>1</sup>H-noise-decoupled <sup>31</sup>P-NMR (121.4 MHz) spectra were obtained with a Varian Unity 300 spectrometer. Typical parameters included a 2,521-Hz sweep width, 4K data points, 4.7 μs pulse (~30° flip angle), 0.8 s recycle time. Free induction decays were processed with 4 Hz line broadening. The temperature was maintained at 25 °C. For the CP spectra, 200–750 transients were collected. CP stock solution (20–100 μL) was added to an enzyme solution with 1 mM catalytic sites at the indicated pH. This covered the range of 2–12 mM CP. To judge the effect of succinate the same experiment was repeated, but with 10 mM succinate present. Chemical shifts for bound ligands were determined from the slope in a plot of  $\delta_{\text{obs}} - \delta_0$ , the chemical shift difference between free CP and that in the presence of enzyme, versus  $E_0/CP_0$ , the total moles of active sites divided by the total moles of CP. The linewidth of the signal for bound ligand in this system was estimated as the slope in a plot of  $\Delta\nu_{\text{obs}} - \Delta\nu_0$  vs.  $E_0/CP_0$ . Errors in estimated linewidths were as much as 20%.

For <sup>31</sup>P-NMR experiments of the catalytic subunit in the presence of PALA, the sweep width was increased to 8,000 Hz (8,000 data points), and the recycle time to 1 s. Approximately 10,000–40,000 transients were collected

and a linebroadening of 4–10 Hz was used. All spectra were referenced to external inorganic phosphate at 0 Hz.<sup>1</sup>

#### Acknowledgments

This work was supported by grants GM26237 (E.R.K.) and GM06920 (W.N.L.) from the National Institute of General Medical Sciences. We thank Dr. S.C. Pastra-Landis and Dr. D. Baker for critically reading this manuscript.

#### References

- Allewell, N.M., Hofmann, G.E., Zaugg, A., & Lennick, M. (1979). Bohr effect in *Escherichia coli* aspartate transcarbamoylase. Linkages between substrate binding, proton binding, and conformational transitions. *Biochemistry* 18, 3008–3015.
- Bethell, M.R., Smith, K.E., White, J.S., & Jones, M.E. (1968). Carbamyl phosphate: An allosteric substrate for aspartate transcarbamoylase of *Escherichia coli*. *Proc. Natl. Acad. Sci. USA* 60, 1442–1449.
- Cohen, R.E. & Schachman, H.K. (1986). Kinetics of the interaction of *N*-(phosphonacetyl)-L-aspartate with the catalytic subunit of aspartate transcarbamoylase. *J. Biol. Chem.* 261, 2623–2631.
- Collins, K.D. & Stark, G.R. (1969). Aspartate transcarbamoylase: Studies of the catalytic subunit by ultraviolet difference spectroscopy. *J. Biol. Chem.* 244, 1869–1877.
- Collins, K.D. & Stark, G.R. (1971). Aspartate transcarbamoylase: Interaction with the transition state analogue *N*-(phosphonacetyl)-L-aspartate. *J. Biol. Chem.* 246, 6599–6605.
- Gerhart, J.C. & Pardee, A.B. (1962). Enzymology of control by feedback inhibition. *J. Biol. Chem.* 237, 891–896.
- Gerhart, J.C. & Pardee, A.B. (1963). The effect of the feedback inhibitor CTP, on subunit interactions in aspartate transcarbamoylase. *Cold Spring Harbor Symp. Quant. Biol.* 28, 491–496.
- Gouaux, J.E., Krause, K.L., & Lipscomb, W.N. (1987). The catalytic mechanism of *Escherichia coli* aspartate carbamoyltransferase: A molecular modelling study. *Biochem. Biophys. Res. Commun.* 142, 893–897.
- Gouaux, J.E. & Lipscomb, W.N. (1988). Three-dimensional structure of carbamyl phosphate and succinate bound to aspartate carbamoyltransferase. *Proc. Natl. Acad. Sci. USA* 85, 4205–4208.
- Gouaux, J.E. & Lipscomb, W.N. (1990). Crystal structures of phosphonoacetamide ligated T and phosphonoacetamide and malonate ligated R states of aspartate carbamoyltransferase at 2.8 Å resolution and neutral pH. *Biochemistry* 29, 389–402.
- Gouaux, J.E., Stevens, R.C., & Lipscomb, W.N. (1990). Crystal structures of aspartate carbamoyltransferase ligated with phosphonoacetamide, malonate and CTP or ATP at 2.8 Å resolution and neutral pH. *Biochemistry* 29, 7702–7715.
- Griffin, J.H., Rosenbusch, J.P., Blout, E.R., & Weber, K. (1973). Conformational changes in aspartate transcarbamoylase: II. Circular dichroism evidence for the involvement of metal ions in allosteric interactions. *J. Biol. Chem.* 248, 5057–5062.
- Griffin, J.H., Rosenbusch, J.P., Weber, K.K., & Blout, E.R. (1972). Conformational changes in aspartate transcarbamoylase. I. Studies of ligand binding and of subunit interactions by circular dichroism spectroscopy. *J. Biol. Chem.* 247, 6482–6490.
- Hamlin, R., Cork, C., Howard, A., Nielson, C., Vernon, W., Mathews, D., & Xuong, N.H. (1981). Characteristics of a flat multiwire area detector for protein crystallography. *J. Appl. Crystallogr.* 14, 85–93.
- Howard, A.J., Nielsen, C., & Xuong, N.H. (1985). Software for a diffractometer with multiwire area detector. *Methods Enzymol.* 114, 452–471.
- Howlett, G.J. & Schachman, H.K. (1977). Allosteric regulation of aspartate transcarbamoylase. Changes in the sedimentation coefficient promoted by the bisubstrate analogue *N*-(phosphonacetyl)-L-aspartate. *Biochemistry* 16, 5077–5083.
- Hsuanyu, Y. & Wedler, F.C. (1987). Kinetic mechanism of native *Esch-*

<sup>1</sup> Inorganic phosphate was not cosolubilized with the enzyme because it binds to the enzyme.

- erichia coli* aspartate transcarbamylase. *Arch. Biochem. Biophys.* 259, 316–330.
- Jones, M.E., Spector, L., & Lipmann, F. (1955). Carbamyl phosphate. The carbamyl donor in enzymatic citrulline synthesis. *J. Am. Chem. Soc.* 77, 819–820.
- Ke, H.-M., Lipscomb, W.N., Cho, Y., & Honzatko, R.B. (1988). Complex of *N*-phosphonacetyl-L-aspartate with aspartate carbamoyltransferase: X-ray refinement, analysis of conformational changes and catalytic and allosteric mechanisms. *J. Mol. Biol.* 204, 725–747.
- Kim, K.H., Pan, Z., Honzatko, R.B., Ke, H.-M., & Lipscomb, W.N. (1987). Structural asymmetry in the CTP-liganded form of aspartate carbamoyltransferase from *Escherichia coli*. *J. Mol. Biol.* 196, 853–875.
- Kirshner, M.W. & Schachman, H.K. (1971). Conformational changes in proteins as measured by difference sedimentation studies. II. Effect of stereospecific ligands on the catalytic subunit of aspartate transcarbamylase. *Biochemistry* 10, 1919–1925.
- Kirshner, M.W. & Schachman, H.K. (1973). Local and gross conformational changes in aspartate transcarbamylase. *Biochemistry* 12, 2997–3004.
- Krause, K.L., Voltz, K.W., & Lipscomb, W.N. (1985). Structure at 2.9-Å resolution of aspartate carbamoyltransferase complexed with the bisubstrate analogue *N*-(phosphonacetyl)-L-aspartate. *Proc. Natl. Acad. Sci. USA* 82, 1643–1647.
- Krause, K.L., Voltz, K.W., & Lipscomb, W.N. (1987). 2.5 Å structure of aspartate carbamoyltransferase complexed with the bisubstrate analog *N*-(phosphonacetyl)-L-aspartate. *J. Mol. Biol.* 193, 527–553.
- Middleton, S.A., Stebbins, J.W., & Kantrowitz, E.R. (1989). A loop involving catalytic chain residues 230–245 is essential for the stabilization of both allosteric forms of *Escherichia coli* aspartate transcarbamoylase. *Biochemistry* 28, 1617–1626.
- Monaco, H.L., Crawford, J.L., & Lipscomb, W.N. (1978). Three-dimensional structures of aspartate carbamoyltransferase from *Escherichia coli* and of its complex with cytidine triphosphate. *Proc. Natl. Acad. Sci. USA* 75, 5276–5280.
- Porter, R.W., Modebe, M.O., & Stark, G.R. (1969). Aspartate transcarbamylase: Kinetic studies of the catalytic subunit. *J. Biol. Chem.* 244, 1846–1859.
- Reichard, P. & Hanshoff, G. (1956). Aspartate carbamyl transferase from *Escherichia coli*. *Acta Chem. Scand.* 10, 548–560.
- Roberts, M.F., Opella, S.G., Schaffer, M.H., Phillips, H.M., & Stark, G.R. (1976). Evidence from carbon-13 NMR for protonation of carbamyl phosphate and PALA in the active site of aspartate transcarbamylase. *J. Biol. Chem.* 251, 5976–5985.
- Robey, E.A. & Schachman, H.K. (1985). Regeneration of active enzyme by formation of hybrids from inactive derivatives: Implications for active sites shared between polypeptide chains of aspartate transcarbamoylase. *Proc. Natl. Acad. Sci. USA* 82, 361–365.
- Robey, E.A., Wente, S.R., Markby, D.W., Flint, A., Yang, Y.R., & Schachman, H.K. (1986). Effect of amino acid substitutions on the catalytic and regulatory properties of aspartate transcarbamoylase. *Proc. Natl. Acad. Sci. USA* 83, 5935–5938.
- Stebbins, J.W., Xu, W., & Kantrowitz, E.R. (1989). Three residues involved in binding and catalysis in the carbamyl phosphate binding site of *Escherichia coli* aspartate transcarbamylase. *Biochemistry* 28, 2592–2600.
- Stebbins, J.W., Zhang, Y., & Kantrowitz, E.R. (1990). The importance of residues Arg-167 and Gln-231 in both the allosteric and catalytic mechanisms of *Escherichia coli* aspartate transcarbamylase. *Biochemistry* 29, 3821–3827.
- Stevens, R.C., Gouaux, J.E., & Lipscomb, W.N. (1990). Structural consequences of effector binding to the T state of aspartate carbamoyltransferase: Crystal structures of the unligated and ATP- and CTP-complexed enzymes at 2.6 Å resolution. *Biochemistry* 29, 7691–7701.
- Stevens, R.C., Reinisch, K.M., & Lipscomb, W.N. (1991). Molecular structure of *Bacillus subtilis* aspartate transcarbamoylase at 3.0 Å resolution. *Proc. Natl. Acad. Sci. USA* 88, 6087–6091.
- Swift, T.J. & Connick, R.E.I. (1962). NMR-relaxation mechanisms of O<sup>17</sup> in aqueous solutions of paramagnetic cations and the lifetime of water molecules in the first coordination sphere. *J. Chem. Phys.* 37, 307–320.
- Wedler, F.C. & Gasser, F.J. (1974). Ordered substrate binding and evidence for a thermally induced change in mechanism for *E. coli* aspartate transcarbamylase. *Arch. Biochem. Biophys.* 163, 57–68.
- Wente, S.R. & Schachman, H.K. (1987). Shared active sites in oligomeric enzymes: Model studies with defective mutants of aspartate transcarbamoylase produced by site-directed mutagenesis. *Proc. Natl. Acad. Sci. USA* 84, 31–35.
- Wild, J.R., Loughrey-Chen, S.J., & Corder, T.S. (1989). In the presence of CTP, UTP becomes an allosteric inhibitor of aspartate transcarbamylase. *Proc. Natl. Acad. Sci. USA* 86, 46–50.
- Xi, X.G., Van Vliet, F., Ladjimi, M.M., Cunin, R., & Hervé, G. (1990). The catalytic site of *Escherichia coli* aspartate transcarbamoylase: Interaction between histidine 134 and the carbonyl group of the substrate carbamyl phosphate. *Biochemistry* 29, 8491–8498.
- Xu, W. & Kantrowitz, E.R. (1989). Function of threonine-55 in the carbamoyl phosphate binding site of *Escherichia coli* aspartate transcarbamoylase. *Biochemistry* 28, 9937–9943.
- Xu, W. & Kantrowitz, E.R. (1991). Function of serine-52 and serine-80 in the catalytic mechanism of *Escherichia coli* aspartate transcarbamoylase. *Biochemistry* 30, 2535–2542.
- Yates, R.A., & Pardee, A.B. (1956). Control of pyrimidine biosynthesis in *Escherichia coli*. *J. Biol. Chem.* 221, 757–770.